Comparative characteristics of power delivery and temperature between conventional and hybrid energy storage systems in UAVs

Prasophchok Phumma[1], *and Waiard Saikong*[2*]

[1]Power Engineering Technology, College of Industrial Technology, King Mongkut's University of Technology North Bangkok, Bangkok 10800, Thailand.
[2]Research Centre for Combustion Technology and Alternative Energy (CTAE), Science and Technology Institute, King Mongkut's University of Technology North Bangkok, Bangkok 10800, Thailand.

Abstract. This research endeavors to present an analysis the characteristics of the power delivery and temperature between conventional energy storage systems (CESS) and hybrid energy storage systems (HESS) to aid in the development of advanced energy storage solutions for Unmanned Aerial Vehicles (UAVs). The results demonstrate that the HESS allows batteries to achieve one additional discharge cycle compared to CESS. Additionally, HESS reduces the initial current response and power delivery by 30W, enabling greater energy consumption efficiency. The average surface temperature differential between the two systems is 1.2°C and the average peak differential is 1.6°C, as the HESS exhibits a slower temperature rise during discharge two cycle to end, due to the initial assistance provided by the supercapacitor and maintain smooth surface peak temperature. The findings highlight the potential for HESS to enhance UAV performance, indicating the need for longer experiment durations, stable room temperatures, and consideration of the mission profile for more accurate data.

1 Introduction

Unmanned aerial vehicles system (UAVs) technology has gained significant prominence across various sectors due to its affordability and ease of control. This trend has led to increasing demand, particularly in applications such as [1]. Large UAVs, capable of carrying heavy payloads, are suitable for a wide range of industries, underscoring the need for a reliable and stable operation to ensure safety [2]. Conventional energy storage systems (CESS), such as primary source Lithium Polymer (Li-Po) batteries with high-power density, are critical in mitigating potential risks in case of accidents. Efficient energy storage systems are essential for maintaining performance and airworthiness. However, these system constraints can restrict flight endurance and payload capacity, leading to excessive energy loss and heat generation [3].

A pure primary source cannot ensure stable performance. Therefore, Hybrid Energy Storage Systems (HESS) combines of multiple energy storage source, such as batteries and supercapacitors to improve performance. Supercapacitors have higher power density to respond to power load in a short time. They are perform a good broad temperature range and maintain temperature environment [4, 5, 6].

The characteristics of power delivery and temperature impact significantly influence the performance of energy storage systems. Evaluating the dynamics of power delivery fluctuations and monitoring temperature variations are critical to ensuring the safety and reliability of these systems, particularly during operational periods. These assessments are essential to optimize system performance, prevent potential failures, and maintain operational efficiency. Understanding these parameters allows for the development of more robust and efficient energy storage solutions, thereby enhancing the overall reliability and safety of the systems in which they are implemented.

The goal of this study is to conduct a thorough analysis of the characteristics of power delivery and temperature characteristics of CESS and HESS for the development of stainable energy storage systems in UAVs. By establishing a robust testing framework, we will evaluate these characteristics to contribute to the development of energy storage systems for UAVs applications.

The paper is structured as follows. In section 2, materials and methodology will present two different systems configurations and testing procedures. Subsequently, in section 3, results and discussion will present comparative analysis of power delivery and temperature characteristics. The final section, conclusion will present nuanced understanding into the dynamics characteristics relationship with capacity level such as voltage, current power and surface temperature of both systems, and perspectives for avenues for future research.

* Corresponding author: waiard.s@cit.kmutnb.ac.th

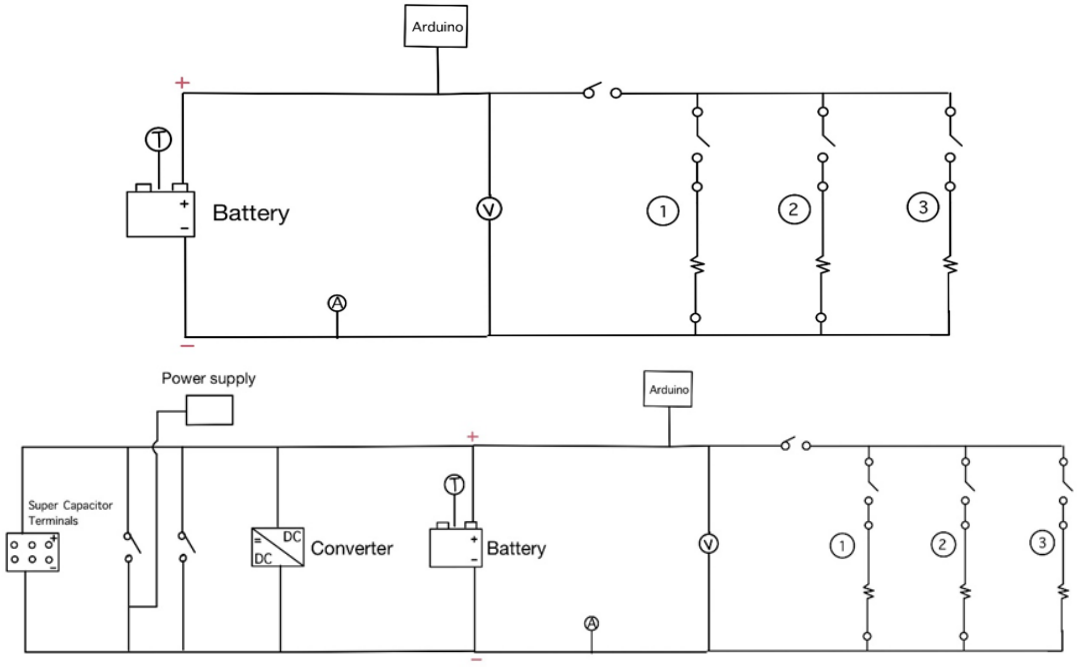

Fig. 1 Energy Storage Systems schematic between CESS (upper) and HESS (lower)

2 Materials and Methodology

2.1 Systems Configuration

For comparison purposes, Fig. 1 schematically depicts the reference ESS similar to [7]. Two systems are evaluated.

Conventional Energy Storage System (CESS):

This system typically relies on energy storage technology. In UAVs requirement reliability and light weight design. Li-Po batteries are commonly used due to high energy density and ability for mission performance. The specifications of the Li-Po batteries are summarized in Table 1.

Hybrid Energy Storage System (HESS):

This system combines Li-Po batteries with a supercapacitor.

The batteries are used as a major energy source, while the supercapacitor module is integrated to handle the delivery power fluctuation. The specifications of the supercapacitor are summarized in Table 2

2.2 Experimental set up

This section provides a setup to simulate static loads for the evaluation of two different systems and to monitor data from the sensor for comparison. The setup consists of the following components:

Dummy Loads Testing: Configurable resistive loads to replicate the varying power requirements encountered during UAVs flight phases. The number of dummy loads required to represent actual consumption specified a discharge rate similar to [8]. Therefore, it is necessary to calculate the total resistance (R) required for the parallel connection with three dummy loads. Using Ohm's Law expressed in equation 1, obtain the specified load.

$$V = IR \tag{1}$$

Arduino Mega 2560 and Sensor module Overview: This study will utilized the Arduino platform was designed to produce devices that can easily engage with the environment and combine three sensors at a low cost. For data collection, of Voltage sensor will measure the output voltage (Vout) from the voltage divider circuit using Arduino's ADC, expressed in equation 2 to solve for the input voltage (Vin) [9]

$$V_{out} = V_{in}*((R_2+R_1)/R_1) \tag{2}$$

The ACS712 sensor detects the load current, converts it to a corresponding voltage level, and sends this data to an Arduino. The Arduino then provides an analog output signal that is a linear representation of the instantaneous current. The calculation for output current is expressed in [10] and the last of sensor is NTC Thermistor will use its changing resistance to measure output temperature by the nonlinear relationship between resistance and temperature (R-T) described a relatively by the Steinhart-Hart equation in [11]. The collected data will be analysed and visualized shown in section 3 to monitor for comparative purposes to study characteristics of power delivery and temperature with the surface temperature and average temperature of the batteries during the operation testing of two different system configurations.

Main Circuit Breaker: used to cut off the power supply from batteries, protecting the system from excessive current or short circuits. A separate circuit with a

dummy load can be used to safely discharge excess power.

2.3 Testing Procedure

Initial Calibration: All sensors and data logging equipment were calibrated to ensure precise and accurate measurements.

Evaluation Systems: As detailed in section 2.1, this consisted of two systems for evaluation, each involving three tests. In each test, the system underwent discharge cycles at a rate of 30 A for 25 seconds. Following discharge, the main circuit breakers for all three dummy loads will be manually turned off to supply on systems. The raw data obtained from the sensor module will be collected by Arduino over a total duration of 60 seconds. After that, a 15-minute rest period, allows the battery's open-circuit voltage and temperature to stabilize before continuing the test. The procedure was repeated the procedure until the batteries could no longer power the system, reaching their cut-off point.

For evaluation, Fig. 2 schematically depicts the reference testing systems frameworks. Initial testing with Conventional System to establish baseline performance metrics for power delivery and temperature. In HESS testing, the supercapacitor was charged by the DC-DC converter before the discharge cycle, the same as previously started. After that rest period allow the battery's open-circuit voltage and temperature to stabilize before continuing the test. The procedure was repeated the procedure without recharging the supercapacitor. It's already charged to its usable level.

Table 1. Specification of the Li-Po batteries

Parameters	Description
Cell configuration	3 series
Full charge voltage	12.6 V (Nominal 11.1 V)
Nominal capacity	2,200 mAh
Specific energy range	150-250 Wh/kg
Operation temperature	−20 °C to 60 °C
Cycle life	300 - 500

Table 2. Specification of Supercapacitor [12]

Parameters	Description
Cell configuration	6 series
Nominal voltage	15 V
Capacitance	16 F
Nominal capacity	2,200 mAh
Specific energy range	5 - 15 Wh/kg
Operation temperature	−40 °C to 60°C/
Cycle life	500-1000

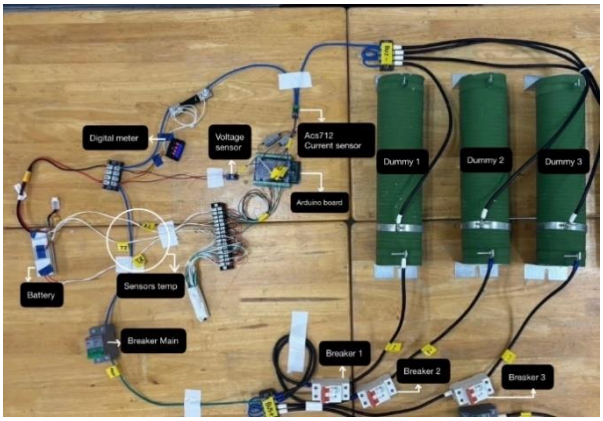

(A)

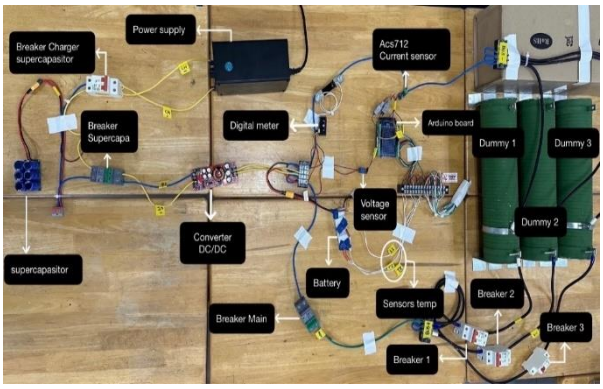

(B)

Fig. 2 Testing Framework between (A) CESS and (B) HESS

3 Results and Discussion

Following the completion of the procedure outlined above and obtain data logging from sensor modules on the Arduino platform, this section presents a comparative analysis and visualization the characteristics of the power delivery and temperature for two different system configurations.

3.1 Power Delivery Analysis

CESS: The results, as shown in Fig. 3A, indicate that the voltage curve characteristic of the relationship between voltage and capacity is usually given in ampere-hours [13]. The amount of current delivered from fully charged at 12.6V gradually decreased until it reached a cut-off average of 8.9V, with an open circuit voltage of 10.7V. The power delivery, in terms of current response to capacity, show that the batteries deliver peak current 34A. They could last for 9 cycles and total discharge capacity of 1.87Ah, as shown in Fig. 4A. The peak power 380Wsteadily decreases in stability over a usage duration of 458 seconds in Fig 5A.

HESS: The results, as shown in Fig. 3B, demonstrate that this system, similar to CESS, contributed to supercapacitor usage. The voltage curve started from a fully charged and dropped cut-off average of 8.3V, with an open circuit voltage of 10V. The current response showed a delivery peak current 30A could last for 10 cycles and a total discharge capacity of 1.91Ah, as shown in Fig. 4B. The average output power was 350W over a

usage duration of 510 seconds, with the curve gradually decreasing and fluctuations as it approaches depletion, as shown in Fig 5B.

3.2 Temperature Analysis

The surface temperature data were collected from three experiments, using different color legends to represent each trial: black for Experiment 1, pink for Experiment 2, and green for Experiment 3. During each cycle of discharging, the temperature rises to a peak and then decreases during the resting period. This analysis includes the results of the average temperature and average peak temperature, calculated from the average of the three experiments.

CESS: The results, as shown in Fig. 6A, indicate a relationship between surface temperature characteristics and battery capacity (Ah). The initial temperature rose from an ambient temperature of 25°C to 29°C during the first cycle. The cumulative average temperature reached 29.97°C and peaked at 34°C when the battery was nearly depleted. The average peak surface temperature was 31.66°C, as shown in Fig. 7A.

HESS: The results, as shown in Fig. 6B, indicate that this system utilizes supercapacitors to assist in power supply before the batteries are discharged. The initial temperature rose from an ambient temperature of 25°C to 27°C during the first cycle. The cumulative average temperature reached 28.76°C and peaked at 32.8°C before the battery ran out. The average surface peak temperature was 30.18°C, as shown in Fig. 7B. The temperature trends for each system are similar to the reported results in [14, 15], remaining within the safe operating range.

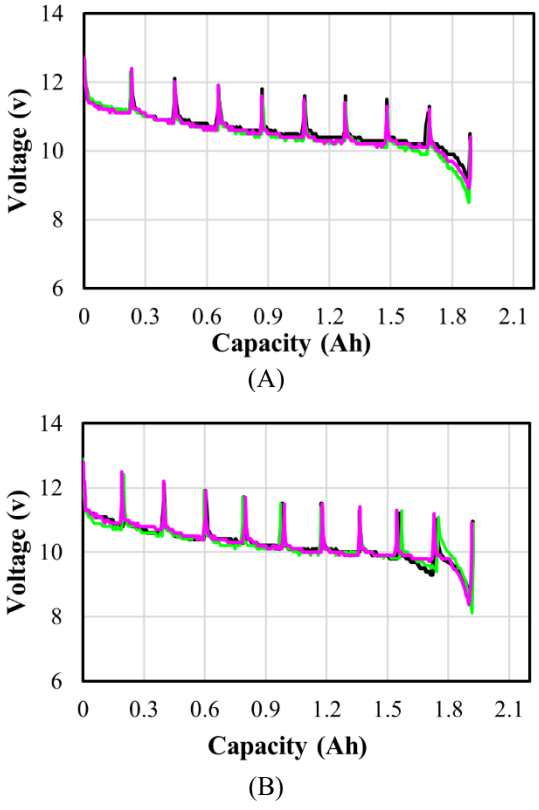

Fig. 3 Voltage characteristic between (A) CESS and (B) HESS

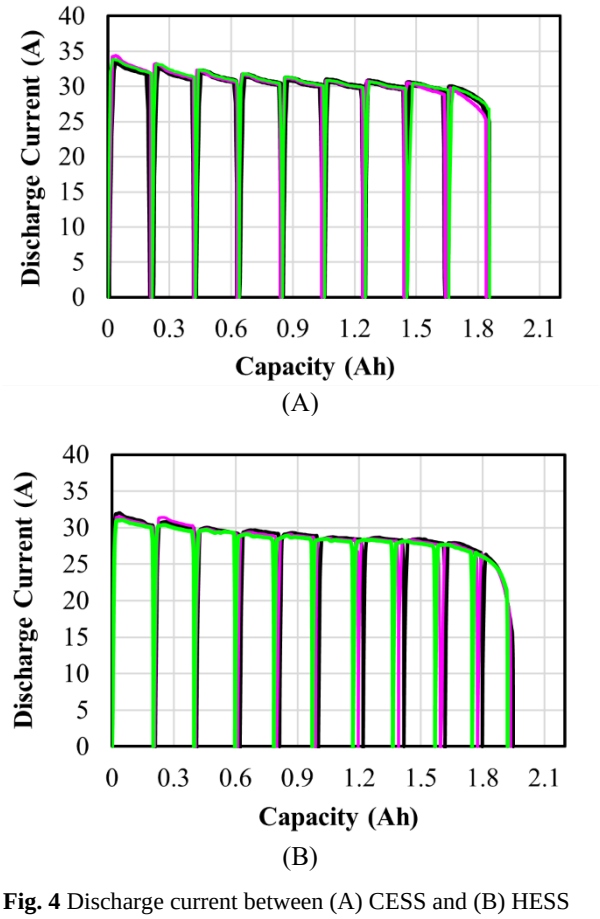

Fig. 4 Discharge current between (A) CESS and (B) HESS

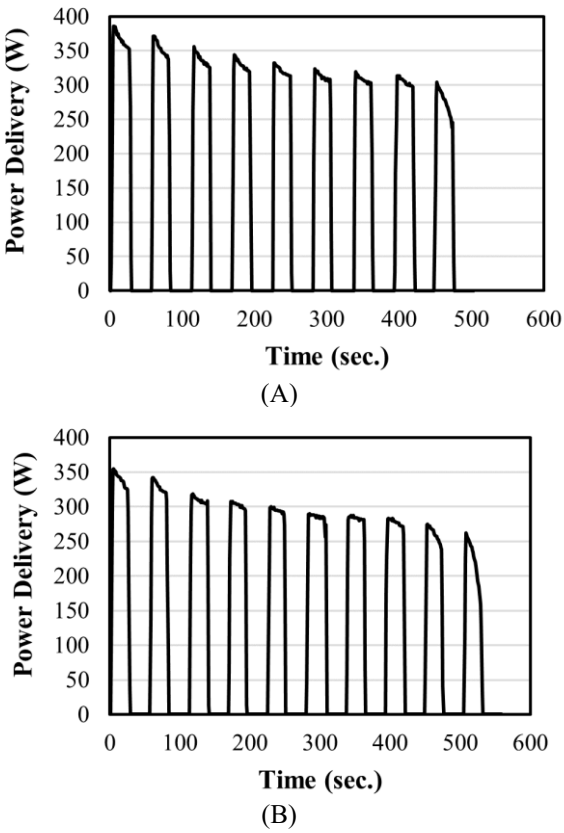

Fig. 5 Power delivery between (A) CESS & (B) HESS

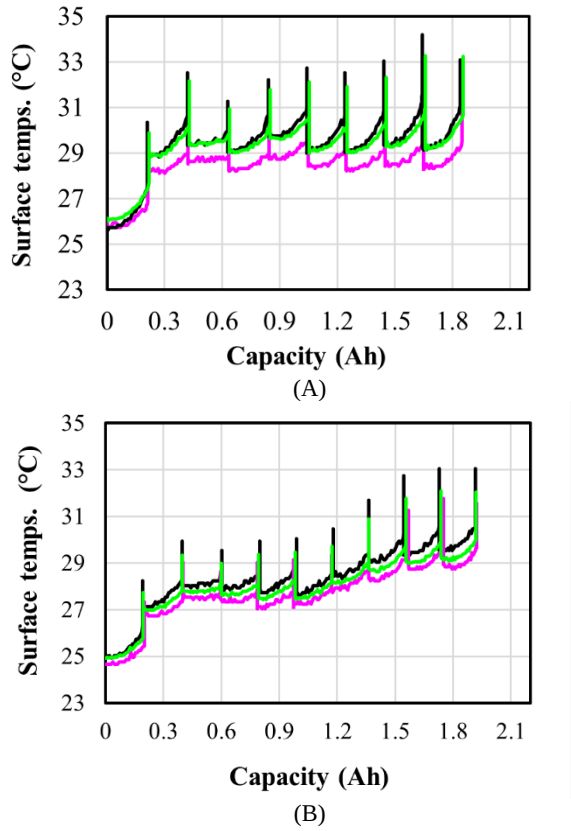

Fig. 6 Surface temperature between (A) CESS and (B) HESS

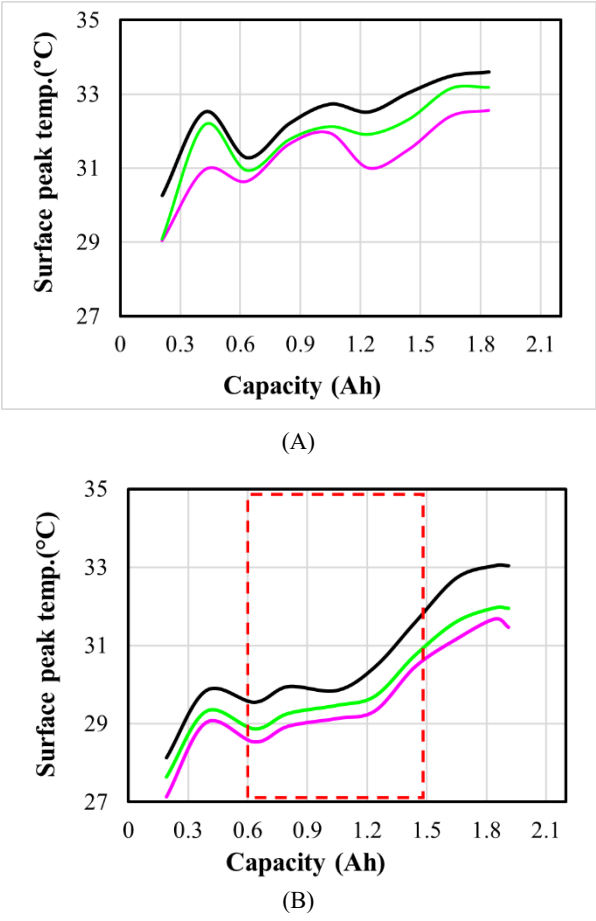

Fig. 7 Surface peak temp. between (A) CESS and (B) HESS

4 Conclusion

In experiments, both CESS and HESS showed similar graph characteristics form the three experiments. However, HESS employs the supercapacitor through a converter to have a higher voltage than the batteries, the supercapacitor initially for a short period before its energy decreases. HESS allows the batteries to be discharged for one cycle longer than CESS. Additionally, HESS reduces the initial current response and power delivery by 30W, enabling greater energy consumption. The surface temperature difference between the two systems is 1.2°C for the average surface temperature and 1.6°C for the average peak temperature. The HESS exhibits a slower temperature rise within a capacity range of 0.6 Ah due to the initial assist from the supercapacitor and maintains a smoother peak temperature compared to the fluctuating CESS, as shown by the red dashed square in Figure 7B.

For future work, the experiment duration should be extended to assess long-term operation and ambient room temperature should be controlled and stabilized to obtain more accurate temperature differences. Additionally, various discharge load should be considered and analysis with the mission profile and real behavior of UAVs when it operates during mission and the control converter should automatically control the voltage level to suit the system's requirements appropriately.

References

1. M. Hassanalian, A. Abdelkefi, Classifications, applications, and design challenges of drones: A review. Progress in Aerospace Sciences, **91**, 99–131, (2017). https://doi.org/10.1016/j.paerosci.2017.04.003
2. Boukoberine, M. N., Zhou, Z., & Benbouzid, M. A critical review on unmanned aerial vehicles power supply and energy management: Solutions, strategies, and prospects. Applied Energy, **255**, 113823. (2019). https://doi.org/10.1016/j.apenergy.2019.113823
3. M. Aneke and M. Wang, Energy storage technologies and real-life applications – A state of the art review. Applied Energy, **179**, 350–377, (2016). https://doi.org/10.1016/j.apenergy.2016.06.097
4. W. Saikong and T. Kulworawanichpong, The Effect of Optimal Vehicle Velocity Trajectory and Optimal Hybrid Energy Storage on Electric Vehicle Energy Consumption, in Proceeding of 2019 Research, Invention, and Innovation Congress (RI2C), Bangkok, Thailand, December 11-13, (2019). https://doi.org/10.1109/RI2C48728.2019.8999922
5. C. Xiao, B. Wang, D. Zhao, and C. Wang, Comprehensive investigation on Lithium batteries for electric and hybrid-electric unmanned aerial vehicle applications. Thermal Science and Engineering Progress, **38**, 101677, (2023). https://doi.org/10.1016/j.tsep.2023.101677

6. C. Zhang et al., A comprehensive review of electrochemical hybrid power supply systems and intelligent energy managements for unmanned aerial vehicles in public services. Energy and AI, **9**, 100175, (2022). https://doi.org/10.1016/j.egyai.2022.100175
7. J. Cao and A. Emadi, A New Battery/UltraCapacitor Hybrid Energy Storage System for Electric, Hybrid, and Plug-In Hybrid Electric Vehicles," in IEEE Transactions on Power Electronics, **27**, 122-132, (2012). https://doi.org/10.1109/TPEL.2011.2151206
8. J. Jaguemont, L. Boulon, and Y. Dubé, A comprehensive review of lithium-ion batteries used in hybrid and electric vehicles at cold temperatures. Applied Energy, **164**, 99–114, (2016). https://doi.org/10.1016/j.apenergy.2015.11.034
9. S. Kazadi, M. Thokozile and K. A. Ogudo, Design and Monitoring of a Voltage battery sensor of an Uninterruptible Power Supply (UPS) by means of an Arduino, in Proceedings of 2020 IEEE PES/IAS PowerAfrica, Nairobi, Kenya, August 25-28, (2020). https://doi.org/10.1109/PowerAfrica49420.2020.9219950
10. R. Khwanrit, S. Kittipiyakul, J. Kudtonagngam and H. Fujita, Accuracy Comparison of Present Low-cost Current Sensors for Building Energy Monitoring, in Proceeding of 2018 ICESIT-ICICTES, Khon Kaen, Thailand, May 7-9, (2018). https://doi.org/10.1109/ICESIT-ICICTES.2018.8442066
11. K. P. S. Rana, V. Kumar, A. K. Dagar, A. Chandel and A. Kataria, FPGA Implementation of Steinhart–Hart Equation for Accurate Thermistor Linearization. IEEE Sensors Journal, **18**, 2260-2267, (2018). https://doi.org/10.1109/JSEN.2018.2795098
12. J. Libich, J. Máca, J. Vondrák, O. Čech, and M. Sedlaříková, Supercapacitors: Properties and applications. Journal of Energy Storage, **17**, 224–227, (2018). https://doi.org/10.1016/j.est.2018.03.012
13. S. Liu, J. Chen, C. Zhang, L. Jin, and Q. Yang, Experimental study on lithium-ion cell characteristics at different discharge rates. Journal of Energy Storage, **45**, 103418, (2022), https://doi.org/10.1016/j.est.2021.103418
14. M. F. H. Rani, Z. M. Razlan, A. B. Shahriman, Z. Ibrahim, and W. K. Wan, Comparative study of surface temperature of lithium-ion polymer cells at different discharging rates by infrared thermography and thermocouple. International Journal of Heat and Mass Transfer, **153**, 119595, (2020). https://doi.org/10.1016/j.ijheatmasstransfer.2020.119595
15. L. Chang et al., Experimental study on the effect of ambient temperature and discharge rate on the temperature field of prismatic batteries, Journal of Energy Storage, **59**, 106577, (2023). https://doi.org/10.1016/j.est.2022.106577